

Mixed Convective Nanofluid Flow with Viscous Dissipation in Surrounding Porous Medium

Md. Nasir Uddin^{1*}, Md. Abdul Alim², Shaikh Reaz Ahmed³

¹(Department of Mathematics, Bangladesh Army University of Engineering & Technology, Natore, Bangladesh)

²(Department of Mathematics, Bangladesh University of Engineering and Technology, Dhaka, Bangladesh)

³(Department of Mechanical Engineering, Bangladesh University of Engineering and Technology, Dhaka, Bangladesh)

*Corresponding Author: Md. Nasir Uddin

ABSTRACT : Heat and mass transfer features with viscous dissipation are studied in a copper-water nanofluid flow through inclined plate in surrounding porous medium. The physical model, namely governing equations is transformed to a dimensionless system as ordinary differential equations whichever are nonlinear via introducing non-dimensional variables. The transformed dimensionless system of equations is solved applying Runge-Kutta integration process of sixth-order together with numerical approach of Nachtsheim and Swigert. Thereafter, comparisons are made with the literature which was published and comparatively acceptable comparisons are reached. The influence of physical parameters as Eckert number, parameters of the fluid suction and Schmidt number are presented upon the flow fields such as in terms of velocity, temperature along with concentration fields including local skin friction coefficient, local Nusselt together with Sherwood numbers. **KEYWORDS:** Mixed convection, nanofluid, porous medium, viscous dissipation.

Date of Submission:08-03-2019

Date of acceptance: 28-03-2019

I. INTRODUCTION

In recent years, nanotechnology has rapid advances to develop of coolants as called nanofluid which are used to enhance the heat transfer rate. Nanofluid is being used for numerous environmental engineering and industrial situations to provide more energy suppliers and other uses such as automobile transmission, boiler exhaust flue gas recovery, cooling of welding, cooling of electronics, drag reductions, engine transmission oil, engine cooling, high-power lasers, heating including cooling of buildings, into diesel electric generator namely jacket water coolant, lubrications, microwave tubes, nuclear reactor, nanofluid in drilling, radiator, refrigeration (domestic refrigerator, chillers), solar water heating, space, thermal storage and so on. Furthermore, others applications are underground coal gasification, food processing, geo-thermal system, and ground water hydrology etc.

Due to wide range of environmental engineering and industrial situations, comparable to the heat transfer, mass transfer also benefited from the use of nanofluid, so over the earlier decade have attracted attention from various research groups to develop complex situations to linear situations. Mixed convection with nanofluid flow through vertical plate has been investigated via Ahmad and Pop [1] within porous medium. The effect of velocity has been considered to present graphically but the results of thermal properties have been neglected for analysis. Non-Darcy steady mixed convection nanofluid flow through horizontal plate has been explored via Rosca et al. [2] within porous medium. The velocity and temperature effects of the field of flow have been presented by graphically neglecting the mass transfer effect on the flow field. For the steady case, mixed convection nanofluid flow within porous medium over inclined plate has been explored via Rana et al. [3]. The standard thermo-physical properties of nanofluid were neglected to analyze by them and there is an opportunity to include these with porous plate. Mixed convection on the flow of nanofluid into porous medium past inclined channel has been reported via Cimpean and Pop [4]. The standard thermo-physical features of nanofluid were considered but ignored the mass transfer effect to analyze by them. Mixed convection and forced-mixed transition of nanofluids flow using thermo physical properties has been analyzed by Feng et al. [5]. The effects of hydro-dynamic together with thermal performance have been included but unkmpt the mass transfer effect for analysis by them. Considering the Soret affects in nanofluid flow, Reddy et al. [6] investigated

heat with mass transfer flow properties in boundary region with mixed convection through vertical plate. Viscous nanofluid flow in velocity and thermal boundary layer region has been reported by Kuppapalle et al. [7]. There are various opportunities to extend this work which was done by Kuppapalle et al. [7]. Thermal effect together with mass stratification for natural convective flow through vertical plate has been investigated via Srinivasacharya and Surender [8]. For mixed convection, impact of thermal radiation with chemical reaction over heat including mass transfer boundary layer flow of nanofluids through stretching/shrinking sheet has been investigated by Pala and Mandal [9] in porous medium. Considering radiation effects, multimedia physical features of nanofluid flow for mixed convection has been reported via Hsiao [10]. Sandeep et al. [11] have studied the heat with mass transfer behaviors with transverse magnetic field in nanofluid flow bygone porous stretching sheet. Analytical together with numerical solutions of unsteady MHD natural convective fluid flow through vertical porous plate together with the impact of thermal radiation as well as Hall current has been explored via Murthya et al. [12]. Doubly stratified mixed convective magneto-hydrodynamic flow of non-Newtonian nanofluid existence with heat generation/ absorption, thermophoresis and Brownian effects has been reported Abbasi et al. [13]. For multi-phase nanofluid, the two dimensional unsteady natural convection flow together with constant heat flux through vertical plate has been investigate via Naraharia et al. [14]. The experimentally investigation of performance of boiling heat transfer on Ethylene Glycol and water based SiO_2 nanofluid has been done by Hu et al. [15]. A numerical comparison of methodology in $\gamma\text{-Al}_2\text{O}_3$ -water flow of nanofluid over and done with sink of aluminum foam heat has been done experimentally by Bayomy and Saghir [16]. Considering the shape effects on nanoparticle and constant magnetic field, the forced convective nanofluid flow of heat transfer has been investigated in porous semi-annulus via Sheikholeslamia and Bhatti [17].

The thought of earlier literatures assessments, to the best of author's knowledge; there is no investigation has been considered as mixed convective nanofluid flow with viscous dissipation in porous medium. Likewise, these types of affects exist in science and technologies as several environmental and man-made industrial engineering fields; due to its uses, the present work is considered to study mixed convective nanofluid flow with viscous dissipation along inclined porous plate in surrounding porous medium on the boundary layer. The governing equations of the flow field are converted into a combination of nonlinear ordinary differential equations via introducing similarity variables and solved numerically. Moreover, for the validity of numerical results, a comparison is made with the literature which is published and comparatively satisfactory comparison is achieved. The impact of various physical features as Eckert number, Schmidt number and fluid suction parameters are presented on the field of flow and analyzed thereafter.

II. MATHEMATICAL ANALYSIS

An incompressible mixed convective nanofluid flow which is laminar and steady through inclined porous plate in porous medium is considered. Moreover, the flow is considered as two dimensional and viscous. The x -axis which is the direction of flow is along the plate and y -axis is normal to the plate together with flow. The velocity components in x and y directions are u and v respectively. The radiation heat flux is negligible in x direction compared with the y direction. Consequently, in the flow field conservation law for mass is obeyed automatically as given below:

$$\frac{\partial u}{\partial x} + \frac{\partial v}{\partial y} = 0 \quad (1)$$

The uniform external velocity of flow field is U_∞ which is parallel to inclined porous plate whereas the porous plate makes angle α to vertical. The symbol g is denoted the gravity due to acceleration. The temperature and concentration of nanofluid within boundary layer are T and C whereas T_w and C_w are wall temperature and concentration of the plate which are greater than ambient temperature T_∞ and concentration C_∞ respectively. The base fluid is considered as water while a nanoparticle is considered as copper (Cu). Moreover, base fluid and nanoparticles by means of nanofluid is in locally thermal equilibrium. The diagram of flow configuration and coordinate system is shown as below in Fig. 1 and thermo physical properties of the base fluid and the nanoparticle are given in Table 1.

Using the present physical features, the modified dimensional boundary layer equations of Pal and Mandal [9] as well as Bachok et al. [18] for the nanofluid flow field in porous medium are expressed in below in term of conservation equations as momentum, energy and concentration:

$$u \frac{\partial u}{\partial x} + v \frac{\partial u}{\partial y} = \nu_{nf} \frac{\partial^2 u}{\partial y^2} + \frac{g}{\rho_{nf}} \left\{ (\rho\beta_t)_{nf} (T - T_\infty) + (\rho\beta_c)_{nf} (C - C_\infty) \right\} \cos \alpha - \frac{\nu_{nf}}{k_{pp}} (u - U_\infty) \quad (2)$$

$$u \frac{\partial T}{\partial x} + v \frac{\partial T}{\partial y} = \alpha_{nf} \frac{\partial^2 T}{\partial y^2} + \frac{\mu_{nf}}{(\rho C_p)_{nf}} \left\{ u \frac{\partial^2 u}{\partial y^2} + \left(\frac{\partial u}{\partial y} \right)^2 \right\} \quad (3)$$

$$u \frac{\partial C}{\partial x} + v \frac{\partial C}{\partial y} = D \frac{\partial^2 C}{\partial y^2} \tag{4}$$

Wherever, ν_{nf} is the kinematic viscosity of the nanofluid, $(\beta_t)_{nf}$ is the coefficient of thermal expansion of nanofluid, $(\beta_c)_{nf}$ is the coefficient concentration expansion of nanofluid, k_{pp} is permeability of the porous medium, α_{nf} is the thermal diffusivity of the nanofluid, μ_{nf} is the effective dynamic viscosity of the nanofluid, ρ_{nf} is the density of the nanofluid, $(\rho C_p)_{nf}$ is the heat capacitance of the nanofluid and D is the mass diffusivity.

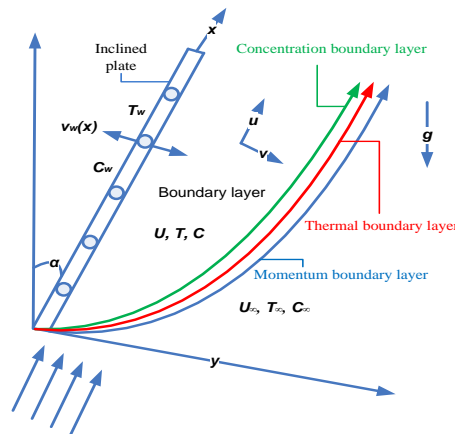


Fig. 1: The diagram of flow configuration

For the nanofluid, effective dynamic viscosity was given via Brinkman [19] as

$$\mu_{nf} = \frac{\mu_{bf}}{(1-\phi)^{2.5}} \tag{5}$$

Where, μ_{bf} is considered as dynamic viscosity of water base fluid and ϕ is considered as nanoparticle solid volume fraction. The relation between physical quantities of base fluid and nanoparticle which were introduced by Abu-Nada [20] are defined as follows:

$$\rho_{nf} = (1-\phi)\rho_{bf} + \phi\rho_{np}, (\rho\beta_t)_{nf} = (1-\phi)(\rho\beta_t)_{bf} + \phi(\rho\beta_t)_{np}, (\rho\beta_c)_{nf} = (1-\phi)(\rho\beta_c)_{bf} + \phi(\rho\beta_c)_{np},$$

$$(\rho C_p)_{nf} = (1-\phi)(\rho C_p)_{bf} + \phi(\rho C_p)_{np}, \nu_{nf} = \frac{\mu_{nf}}{\rho_{nf}}, \frac{K_{nf}}{K_{bf}} = \frac{(K_{np} + 2K_{bf}) - 2\phi(K_{bf} - K_{np})}{(K_{np} + 2K_{bf}) + \phi(K_{bf} - K_{np})}$$

and $\alpha_{nf} = \frac{K_{nf}}{(\rho C_p)_{nf}} \tag{6}$

Wherever, the subscripts *bf* and *np* represent the base fluid and nanoparticle respectively. The boundary conditions which are considered for the current nanofluid flow field are as follows:

$$u = 0, v = \pm v_w(x), T = T_w \text{ and } C = C_w \text{ at } y = 0 \tag{7}$$

$$u = U_\infty, T = T_\infty, \text{ and } C = C_\infty \text{ at } y \rightarrow \infty \tag{8}$$

Where, the subscripts *w* and ∞ denote wall and boundary layer edges respectively whereas the permeability of porous plate is as $v_w(x)$ which is for suction (< 0) or blowing (> 0). It is more convenient to consider the stream function such that equation of continuity is satisfied by the relation:

$$u = \frac{\partial \psi}{\partial y} \text{ and } v = -\frac{\partial \psi}{\partial x} \tag{9}$$

The following dimensionless quantities which were introduced via Cebeci et al. [21] are used to reduce the complexity of the current nanofluid flow field:

$$\eta = y \sqrt{\frac{U_\infty}{\nu_{bf} x}}, \psi = \sqrt{\nu_{bf} x U_\infty} f(\eta), \theta(\eta) = \frac{T - T_\infty}{T_w - T_\infty} \text{ and } s(\eta) = \frac{C - C_\infty}{C_w - C_\infty} \tag{10}$$

By applying the above mentioned dimensionless quantities into Eqn. (13) and transformed equation can

be written as:

$$u = U_\infty f'(\eta) \text{ and } v = \frac{1}{2} \sqrt{\frac{v_{bf} U_\infty}{x}} [\eta f'(\eta) - f(\eta)] \tag{11}$$

Wherever, the prime denotes differentiation with respect to η .

Moreover others dimensional Eqn. (2)-(4) are transformed in terms of momentum, energy and concentration equations using dimensionless quantities are as follows:

$$f''' + \phi_1 \left\{ \frac{1}{2} \phi_2 f f'' + (\phi_3 Ri_t \theta + \phi_4 Ri_c s) \cos \alpha \right\} + K(1 - f') = 0 \tag{12}$$

$$\theta'' + \frac{1}{2} \left(\frac{Pr}{\phi_5} \right) \left\{ \phi_6 f \theta' + \frac{2}{\phi_1} Ec (f' f''' + f''^2) \right\} = 0 \tag{13}$$

$$s'' + \frac{1}{2} Sc f s' = 0 \tag{14}$$

together with the corresponding boundary conditions are given below:

$$f = f_w, f' = 0, \theta = 1, s = 1, \text{ at } \eta = 0 \tag{15}$$

$$f' \rightarrow 1, \theta \rightarrow 0 \text{ and } s \rightarrow 0 \text{ at } \eta \rightarrow \infty \tag{16}$$

In the above Eqn. (15), $f_w = -v_w(x) \sqrt{\frac{x}{v_{bf} U_\infty}}$ is the wall mass transfer coefficient as $f_w > 0$ for suction

and $f_w < 0$ for injection or blowing. In the above dimensionless Eqns. (12)-(14), the physical parameters are defined as below:

$$Gr_t = \frac{g(\beta_t)_{bf} (T_w - T_\infty) x^3}{v_{bf}^2}, Gr_c = \frac{g(\beta_c)_{bf} (C_w - C_\infty) x^3}{v_{bf}^2}, Re_x = \frac{x U_\infty}{v_{bf}}, Ri_t = \frac{Gr_t}{(Re)^2}, Ri_c = \frac{Gr_c}{(Re)^2},$$

$$K = \frac{x v_{bf}}{k_{pp} U_\infty}, Pr = \frac{v_{bf} (\rho C_p)_{bf}}{K_{bf}}, Ec = \frac{U_\infty^2}{(C_p)_{bf} (T_w - T_\infty)}, Sc = \frac{v_{bf}}{D}, \phi_1 = (1 - \phi)^{2.5}, \phi_2 = (1 - \phi) + \phi \frac{\rho_{np}}{\rho_{bf}}$$

$$\phi_3 = (1 - \phi) + \phi \frac{(\rho \beta_t)_{np}}{(\rho \beta_t)_{bf}}, \phi_4 = (1 - \phi) + \phi \frac{(\rho \beta_t)_{np}}{(\rho \beta_t)_{bf}}, \phi_5 = \frac{K_{nf}}{K_{bf}} \text{ and } \phi_6 = (1 - \phi) + \phi \frac{(\rho C_p)_{np}}{(\rho C_p)_{bf}} \tag{17}$$

Wherever in Eqn. (20), Gr_t is the local thermal Grashof number, Gr_c is the local mass Grashof number, Re_x the local Reynolds number, Ri_t is the local Richardson number of thermal, Ri_c is the local Richardson number of mass, K is the parameter of permeability, Pr is the Prandtl number, Ec is the Eckert number and Sc is the Schmidt number whereas $\phi_i (i = 1, \dots, 6)$ are constants.

The physical parameters which are the practical interest are skin-friction coefficient, the local Nusselt and the Sherwood numbers. By employing definition of wall shear stress $\tau_w = \mu_{nf} (\partial u / \partial y)_{y=0}$ along with Fourier's law $q_w = -k_{nf} (\partial T / \partial y)_{y=0}$ and Fick's law $q_m = -D (\partial C / \partial y)_{y=0}$ the non-dimensional forms of local skin-friction coefficient is $C_f = (2 / \phi_1) Re_x^{-1/2} f''(0)$, local Nusselt number is $Nu_x = -\phi_5 Re_x^{1/2} \theta'(0)$ and local Sherwood number is $Sh = -Re_x^{1/2} s'(0)$.

Table 1 Thermo physical properties of base and nanoparticle

Thermo Physical Properties	Base Fluid (Water, H ₂ O)	Copper (Cu)
ρ (kg/m ³)	997.1	8933
C_p (J/kg K)	4179	385
k (W/m K)	0.613	401
$\beta \times 10^{-3}$ (1/K)	21	1.67

III. SOLUTION PROCEDURES

The multifaceted flow configuration is converted into combination as partial differential equations together with boundary conditions. These converted equations are transformed as ordinary differential equations which are dimensionless as well as nonlinear with boundary conditions using appropriate similarity variables. Nachtsheim and Swigert [22] was introduced shooting technique which is used to find unspecific initial

conditions. The transformed boundary value system is converted into initial value system employing Nachtsheim and Swigert [22] approaches. Furthermore, the obtained initial value system is resolved numerically using Runge-Kutta approaches. Moreover, due to obtain well results, sixth order Runge-Kutta approaches is considered to resolve numerically.

IV. COMPARISON

The transfer of dynamic and thermal characteristics for nanofluid flow on fixed or moving flat plate has been investigated via Bachok et al. [18]. The physical characteristics which were considered by them are transferred to mathematical form and then transferred to system of dimensionless ordinary differential equations which were nonlinear. Moreover the system of transformed equations was solved numerically for various physical features with three categories of nanofluid as alumina (Al_2O_3)-water, copper (Cu)-water and titania (Al_2O_3)-water. The numerical results were presented in graphical and tabular forms by them. For the development of the present work, the system of nonlinear as well as dimensionless ordinary differential equations which was considered by Bachok et al. [18] is solved numerically applying numerical approach of Nachtsheim and Swigert [22].

Thereafter, comparisons are carried out as the actual results of Bachok et al. [18] which were published together with the verified of Bachok et al. [18] work. The Fig. 2 show the comparison as the influence of nanoparticle volume fraction ϕ on the velocity field for copper (Cu)-water nanofluid with Prandtl number as $\text{Pr} = 6.2$ and velocity ratio parameter as $\lambda = -0.4$. The numerical results like as first solution of Bachok et al. [18] work are found excellent agreement with the velocity variations. This acceptable comparison indication is to develop the numerical approach of Nachtsheim and Swigert [22] for the present work. Moreover, the numerical results for the present work will report into next following section and analyze thereafter.

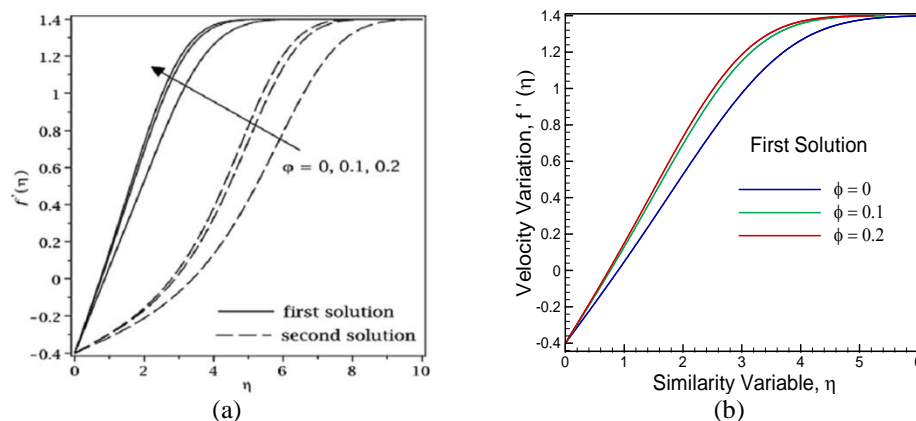


Fig. 2: Comparison of first solution of velocity variation between (a) actual results of Bachok et al. [18] and (b) verified of Bachok et al. [18] work for nanoparticle volume fraction ϕ with $\text{Pr} = 6.2$ and $\lambda = -0.4$ using copper (Cu)-water nanofluid

V. RESULTS AND DISCUSSIONS

The numerical results which are obtained for copper (Cu) - water nanofluid flow of heat together with mass transfers as velocity, temperature together with concentration fields are computed by employing the values of nondimensional parameters $Ri_t = 1.0$, $Ri_c = 1.0$, $K = 0.5$, $\alpha = 30^\circ$, $\text{Pr} = 6.2$, $Ec = 1.0$, $Sc = 0.60$, $f_w = 1.5$, $\phi = 0.03$ and $U_\infty / v = 1.0$ except otherwise specified. The thermo physical properties of nanoparticle are considered for copper (Cu) and water as base fluid of the fluid flow.

The impact of Eckert number Ec ($Ec = 0, 1, \text{ and } 2$) on dimensionless velocity, temperature together with concentration are presented in Figs. 3(a) – 3(c). The uniform external velocity of flow field increases together with increase of Eckert number Ec as a result the velocity difference between the wall and free stream of the flow field increases; therefore the velocity of the field of flow decreases as in Fig. 3(a). The heat dissipation potential of flow field decreases together with the increase of Ec number that's why temperature of the field of flow decrease whereas concentration increases insignificantly because Ec number has insignificantly effects on concentration of the flow field as in Figs. 3(b) – 3(c). Moreover, skin friction coefficient with local Nusselt and local Sherwood numbers for nanofluid flow of Cu-water flow with variation of Eckert number Ec are presented by Figs. 4(a) – 4(c). As enhance of Eckert number Ec ; wall shear stress of the field of flow reduces as a result skin friction coefficient C_f in conjunction with local Sherwood number Sh and local Nusselt number Nu_x reduces for copper (Cu) and water nanofluid as Figs. 4(a) – 4(c).

The impacts of fluid suction of copper-water nanofluid flow on velocity, temperature in addition to concentration boundary layer thickness are shown in Figs. 5(a) – 5(c) for suction parameter f_w ($f_w = 1.5, 2.5$ and 3.5). It is observed as velocity variation in Fig. 5(a), the hydrodynamic boundary layer thickness such as velocity increases adjacent the plate because when the fluid suction starts; the nanofluid passes through the plate which causes a velocity. However, after the adjacent layer, velocity of nanofluid flow field decreases for the increase of fluid suction of the nanofluid due to the fluid suction through the plate increases, the plate is cooled down and the viscosity of the flowing nanofluid flow increases. Therefore, velocity of nanofluid flow field decreases as the fluid suction increases of the nanofluid. Moreover thermal boundary layer thickness as temperature which is exhibited in Fig. 5(b) of nanofluid flow field decreases adjacent to the plate because the plate is cooled down due to fluid suction through the plate increases. But, since the wall temperature is greater than the ambient temperature, the wall reduces heat into nanofluid and the temperature of the nanofluid increases after the adjacent layer of wall and finally convergences to boundary condition. In Fig. 5(c), it is observed that concentration boundary layer thickness as concentration of the nanofluid flow field at all points decreases for the reason that more nanofluid passes through the plate as the fluid suction of nanofluid increases. However, the local skin friction coefficient C_f increases together with the fluid suction increases causing the viscosity of the flowing fluid increases at the plate which is observed in Fig. 6(a). Figures 6(b) – 6(c) depict the local Nusselt number Nu_x and the local Sherwood number Sh against the streamwise distance x . The local Nusselt number and the local Sherwood number increase with the increase of fluid suction parameter due to increase in temperature and decrease in concentration difference respectively, which is shown in Figs. 6(b) – 6(c).

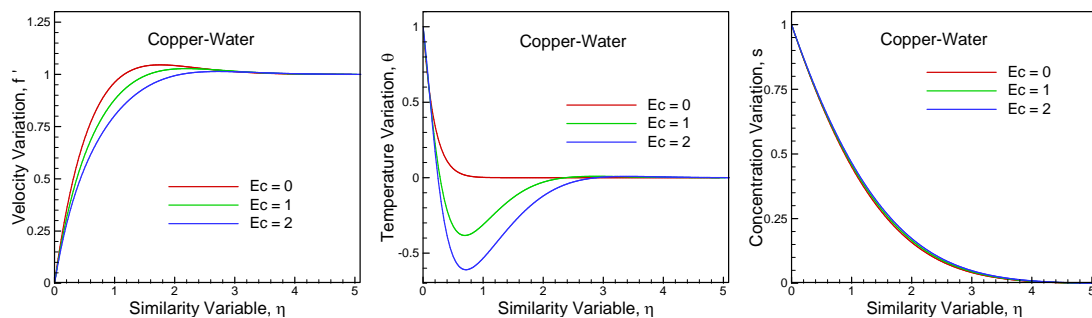


Fig. 3: Variation of (a) velocity; (b) temperature; (c) concentration for effect of Eckert number Ec

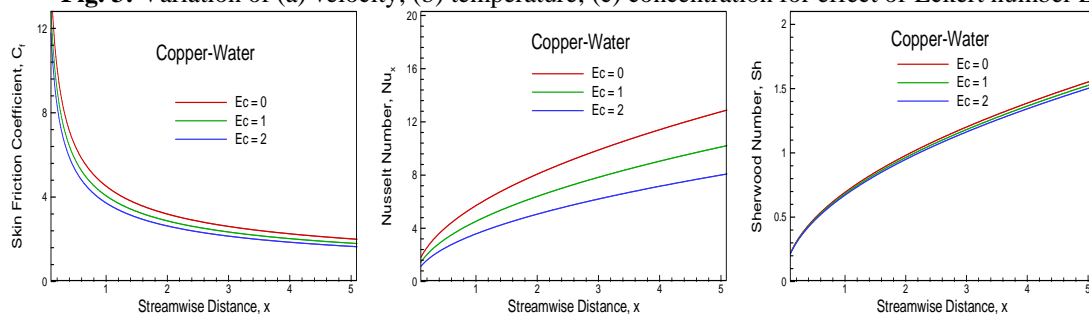


Fig. 4: Effects of Eckert number Ec on (a) local skin friction coefficient; (b) local Nusselt number; (c) local Sherwood number against the streamwise distance

The behavior of the Schmidt number Sc for $Sc = 0.22, 0.60$ and 0.94 on the nanofluid flow as consideration of hydrodynamic, thermal and concentration boundary layer thicknesses of the nanofluid flow are observed via Figs. 7(a) – 7(c). From the Fig. 7(a), it is observed that hydrodynamic boundary layer thickness i.e. velocity of the nanofluid flow field reduces with the raise of Schmidt number due to increase of kinematic viscosity for increase of Schmidt number. Adjacent to the wall, temperature of the nanofluid flow increases because the wall temperature is greater than the ambient temperature of the field of flow and after the adjacent layer of near the wall, temperature of the nanofluid decreases and finally convergences to boundary condition as in Fig. 7(b). With the increases of Schmidt number, the mass diffusivity of the nanofluid flow decreases consequently the concentration of the field of flow decreases, this is observed via Fig. 7(c). From the observation of velocity variation, as expected local skin friction coefficient C_f decreases affecting the local shear stress of the flowing fluid decreases at the plate together with the Schmidt number Sc increases which is observed in Fig. 8(a). Nevertheless, the local Nusselt number Nu_x and the local Sherwood number Sh against the streamwise distance x increase with the increase of Schmidt number Sc due to increase in heat and mass flux respectively, which are shown by Figs. 8(b) – 8(c).

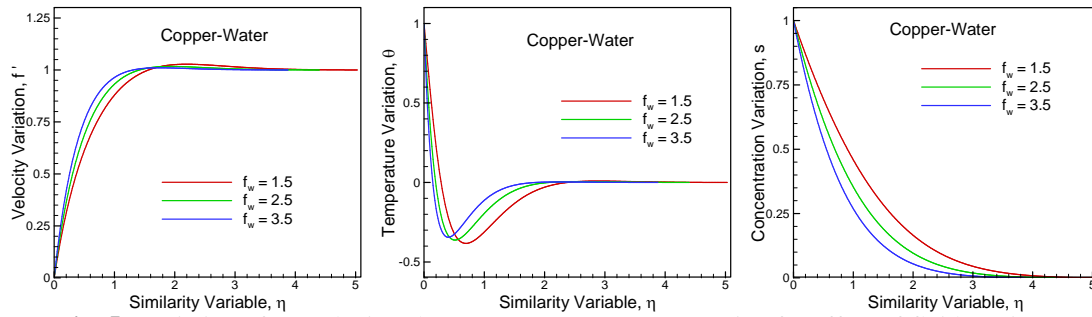


Fig. 5: Variation of (a) velocity; (b) temperature; (c) concentration for effect of fluid suction f_w

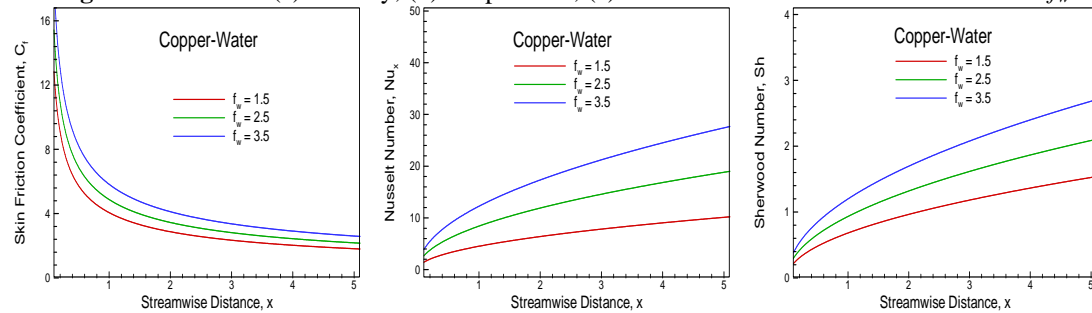


Fig. 6: Effects of fluid suction f_w on (a) local skin friction coefficient; (b) local Nusselt number; (c) local Sherwood number against the streamwise distance

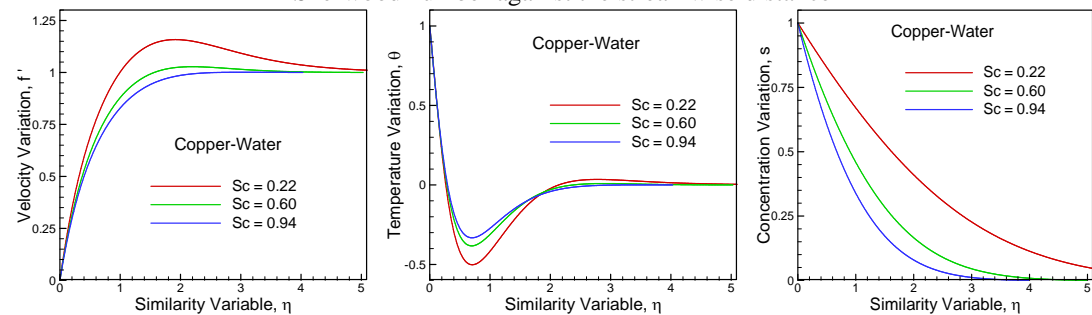


Fig. 7: Variation of (a) velocity; (b) temperature; (c) concentration for effect of Schmidt number Sc

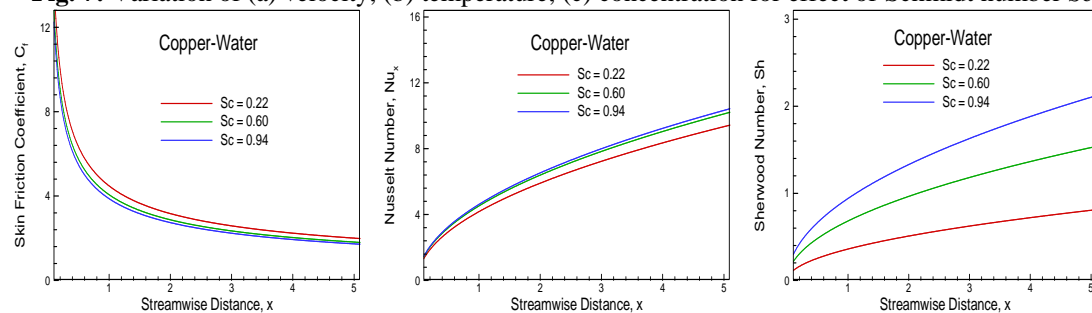


Fig. 8: Effects of Schmidt number Sc on (a) local skin friction coefficient; (b) local Nusselt number; (c) local Sherwood number against the streamwise distance

VI. CONCLUSION

Mixed convective nanofluid flow with viscous dissipation along inclined porous plate in surrounding porous medium has been investigated. The physical flow configuration of this investigation is transformed into combination of mathematical model as partial differential equations together with boundary conditions. The mathematical model as boundary layer approximations are transformed into nonlinear boundary layer equations using appropriate similarity variables. The transformed boundary value system is converted into initial value system employing Nachtsheim and Swigert [22] approaches together with sixth-order Runge-Kutta integration scheme and solved numerically. Thereafter, comparisons of numerical results are prepared as the actual results of Bachok et al. [18] which was published together with the verified of Bachok et al. [18] work and comparatively acceptable comparisons is reached. The numerical results are presented for the effects of Eckert number Ec , parameters of the fluid suction f_w , Schmidt number Sc and nanoparticles volume fraction ϕ on the flow field. From the present investigation, the resulting conclusions can be written on velocity, temperature

together with concentration fields as well as local skin friction coefficient C_f and local Nusselt number Nu_x together with local Sherwood number Sh are as follows:

- Due to increase of Eckert number, the velocity and temperature decrease while concentration of the flow field increases slightly. However, wall shear stress as like local skin friction coefficient, rate of heat transfer as like local Nusselt number together with rate of mass transfer as like local Sherwood number decrease by increase of Eckert number.
- It is seen that increasing fluid suction has the effect to increase the velocity together with temperature into adjacent boundary but decreases in the next and converges to boundary condition while temperature decreases adjacent to the boundary but increases in the next and converges to boundary condition. Moreover concentration of the flow field decreases whereas increase the wall shear stress as like local skin friction coefficient, the rate of heat transfer as like local Nusselt number together with the rate of mass transfer as like local Sherwood number.
- Both the velocity and concentration of the flow field decrease significantly with increase of Schmidt number, consequently local skin friction coefficient decreases although local Sherwood number increases. Moreover, the temperature increases into adjacent boundary but decreases in the next and converges to boundary condition with the increase of Schmidt number, however local Nusselt number increases due to increase of Schmidt number.

REFERENCES

- [1]. Ahmad, S. and Pop, I., Mixed convection boundary layer flow from a vertical flat plate embedded in a porous medium filled with nanofluids, *International Communications of Heat and Mass Transfer* 37, 987-991 (2010).
- [2]. Rosca, A.V., Rosca, N. C., Grosan, T. and Pop, I. Non-Darcy mixed convection from a horizontal plate embedded in a nanofluid saturated porous media, *International Communications of Heat and Mass Transfer* 39, 1080-1085 (2012).
- [3]. Rana, P., Bhargava, R. and Beg, O. A., Numerical solution for mixed convection boundary layer flow of a nanofluid along an inclined plate embedded in a porous medium, *Computer and Mathematics with Applications* 64, 2816-2832 (2012).
- [4]. Cimpean, D. S. and Pop, I., Fully developed mixed convection flow of a nanofluid through an inclined channel filled with a porous medium, *International Journal of Heat and Mass Transfer* 55, 907-914 (2012).
- [5]. Feng, Z., Luo, Z., Zhu, H., Fang, Z. and Li, W., Thermophysical property-based evaluation of mixed convection performance and criteria of forced-mixed transition for nanofluids, *International Journal of Heat and Mass Transfer* 62, 214-222 (2013).
- [6]. Reddy, C. R., Murthy, P. V. S. N., Chamkha, A. J. and Rashad, A. M., Soret effect on mixed convection flow in a nanofluid under convective boundary condition, *International Journal of Heat and Mass Transfer* 64, 384-392 (2013).
- [7]. Kuppapalle, V., Vinayaka, P. K. and Chiu-On, N., The effect of variable viscosity on the flow and heat transfer of a viscous Ag-water and Cu-water nanofluids, *Journal of Hydrodynamics* 25(1), 1-9 (2013).
- [8]. Srinivasacharya, D. and Surender, O., Non-similar solution for natural convective boundary layer flow of a nanofluid past a vertical embedded in a doubly stratified porous medium, *International Journal of Heat and Mass Transfer* 71, 431-438 (2014).
- [9]. Pala, D. and Mandal, G., Influence of thermal radiation on mixed convection heat and mass transfer stagnation-point flow in nanofluids over stretching/shrinking sheet in a porous medium with chemical reaction, *Nuclear Engineering and Design* 273, 644-652 (2014).
- [10]. Hsiao, K. L., Nanofluid flow with multimedia physical features for conjugate mixed convection and radiation, *Computer & Fluids* 104, 1-8 (2014).
- [11]. Sandeep, N., Kumar, B. R. and Kumar, M. S. J., A comparative study of convective heat and mass transfer in non-Newtonian nanofluid flow past a permeable stretching sheet, *Journal of Molecular Liquids* 212, 585-591 (2015).
- [12]. Murthya, M. V. R., Raju, R. S. and Rao, J. A., Heat and mass transfer effects on MHD natural convection flow past an infinite vertical porous plate with thermal radiation and hall current, *Procedia Engineering* 127, 1330-1337 (2015).
- [13]. Abbasi, F. M., Shehzad, S. A., Hayat, T. and Ahmad, B., Doubly stratified mixed convection flow of Maxwell nanofluid with heat generation/absorption, *Journal of Magnetism and Magnetic Materials* 404, 159-165 (2016).
- [14]. Naraharia, M., Raju, S. S. K. and Pendyala, R., Unsteady natural convection flow of multi-phase nanofluid past a vertical plate with constant heat flux, *Chemical Engineering Science* 167, 229-241 (2017).
- [15]. Hu, Y., Li, H., He, Y., Liu, Z. and Zaho, Y., Effect of nanoparticle size and concentration on boiling performance of SiO₂-nanofluid, *International Journal of Heat and Mass Transfer* 107, 820-828 (2017).
- [16]. Bayomy, A. M. and Saghir, M. Z., Experimental study of using γ -Al₂O₃-water nanofluid flow through aluminum foam heat sink: Comparison with numerical approach, *International Journal of Heat and Mass Transfer* 107, 181-203 (2017).
- [17]. Sheikholeslamia, M. and Bhatti, M. M., Forced convection of nanofluid in presence of constant magnetic field considering shape effects of nanoparticles, *International Journal of Heat and Mass Transfer* 111, 1039-1049 (2017).
- [18]. Bachok, N., Ishak, A. and Pop, I., Flow and heat transfer characteristic on a moving plate in a nanofluid, *International Journal of Heat and Mass Transfer* 55, 642-648 (2012).
- [19]. Brinkman, H. C. The viscosity of concentrated suspension and solution, *The Journal of Chemical Physics*, 20, 1952, pp. 571-581.
- [20]. Abu-Nada, E. Application of nanofluids for heat transfer enhancement of separated floes encountered in a backward facing step, *International Journal of Heat and Fluid Flow* 29, 242-249 (2008).
- [21]. Cebeci, T. and Bradshaw, P. *Physical and computational aspects of convective heat transfer*, New York, Springer, 1984.
- [22]. Nachtsheim, P. R. and Swigert, P. Satisfaction of asymptotic boundary conditions in numerical solution of systems of nonlinear equations of boundary-layer type, *NASA TND 3004* (1965).

Md. Nasir Uddin "Mixed Convective Nanofluid Flow with Viscous Dissipation in Surrounding Porous Medium" *American Journal of Engineering Research (AJER)*, vol.8, no.03, 2019, pp.299-306